Determination of best groyne combination for mitigating bank erosion

Kaushik Bora and Hriday Mani Kalita

ABSTRACT

This paper presents a novel approach for determining the best combination of groynes in terms of their number, lengths and positions for controlling bank erosion. The vulnerable bank is considered to be protected if a very small value of water flow speed is achieved on the near bank area. A linked simulation–optimization model is developed in this regard which minimizes the total construction cost of the groyne project. At the same time, a constraint in terms of low flow speed in a predefined zone is incorporated, which helps in bank erosion prevention. In the simulation model, the depth-averaged shallow water equations are solved using a finite difference scheme. The optimization problem is formulated in three different approaches to tackle different types of *in situ* field problems. Genetic algorithm (GA) is used to solve the optimization problem. The proposed optimization model is used in two hypothetical test cases including one straight channel and one meandering channel. The results obtained with all the three formulations are found to be logical and establish the potential of the present model for application in real cases.

Key words | finite difference method, genetic algorithm, groyne, shallow water equations, simulation–optimization model

Kaushik Bora
Hriday Mani Kalita (corresponding author)
Department of Civil Engineering,
National Institute of Technology Meghalaya,
Shillong 793003,
India
E-mail: *hridaymanikalita@gmail.com*

INTRODUCTION

Any structure constructed within a river for guiding or managing the flow of the river to make the flow beneficial for mankind is termed as river training structure. Groyne (or spur dike) is one such popular and widely used river training structure. These are some solid structures which are constructed from the river bank and extend towards the main channel flow. They are often constructed with a variety of objectives, such as deflecting the flow away from the vulnerable river bank, enhancing the main channel depth for aid in smooth navigation, promoting sedimentation on required areas, etc. However, for better performances they are often constructed in series but not individually (Alauddin & Tsujimoto 2012). Moreover, construction of such types of structure also requires a high quantity of quality materials. Therefore, caution should always be taken while deciding their optimal set so as to reduce the overall cost of the whole project, at the same time achieving the desired training of the river. This necessitates a prior modelling study to determine the best combination of groynes in terms of their number, length, position, etc., prior to their construction.

Flow simulation around groynes is an important and challenging topic in water resources engineering. Researchers have continuously been making efforts in the last several decades in this regard. Ahmad (1953) conducted one of the pioneer experimental studies for flow simulation around a groyne and proposed an equation for maximum scour depth in terms of the unit discharge. Since then, many studies have been reported in the literature for experimental (Garde *et al.* 1961; Rajaratnam & Nwachukwu 1983; Sukhodolov *et al.* 2004; Yossef & de Vriend 2010;

doi: 10.2166/hydro.2019.151

Sukhodolov 2014; Qin *et al.* 2017; Jeon *et al.* 2018; Juez *et al.* 2018a, 2018b) and numerical (Tingsanchali & Maheswaran 1990; Ouillon & Dartus 1997; Duan & Nanda 2006; McCoy *et al.* 2008; Ouro *et al.* 2016; Glas *et al.* 2018) flow simulation near groynes.

Review of the literature reveals that even though a large volume of studies is available for flow simulation around groynes, very few researchers tried to determine the best combination of groynes. Kuhnle *et al.* (2002) did one of the first such studies to determine the optimal design parameters for groynes. From their experimental study they concluded that a groyne with an orientation angle of 135° with the downstream leads to maximum volume of scour, leading to a good environment for aquatic habitat. Uijttewaal (2005) experimentally compared performances of four sets of groynes (standard reference groynes; groynes with a head having a gentle slope and extending into the main channel; permeable groynes consisting of pile rows; and hybrid groynes consisting of a lowered impermeable groyne with a pile row on top), with each set composed of five identical groynes. He simulated all of these combinations separately and observed that with the second and third type of groyne system the shear stress and the turbulence can be minimized more in comparison to the first type. Mukherjee & Sarma (2010) determined the best combination of groynes to be applied for a vulnerable reach of the River Brahmaputra in India. They created a variety of combinations by changing the number, position and length of the groynes and numerically simulated each combination separately. Finally, from the comparative analysis, they proposed the best combination to save the vulnerable river bank. Alauddin & Tsujimoto (2012) did another numerical study to determine the best combination of groynes for three key features: scour depth near groynes for structural stability; deposition near the bank for bank safety; and erosion in the main channel bed for navigability. Their results revealed that groynes with parabolic orientation with an average angle of 110° with the upstream are the best for the stated targets. Hakimzadeh *et al.* (2012) stated that the local scour around a groyne can be minimized by using a sloped wall groyne. Their experimental results revealed that using a groyne with lateral slope angle of 83.945°, the maximum scour depth can be minimized by 22.23% and volume of scour hole can be minimized by 60% in comparison to the vertical side wall groyne. Tritthart *et al.* (2014) developed a three-dimensional (3D) numerical model for a reach of the River Danube in Austria and found the best combination which gives the desired effect on flow field as well as morphodynamic and ecological conditions. Karmaker & Dutta (2016) tried to determine the best combination of groynes in terms of their number, length and position for a vulnerable reach of the River Brahmaputra in India. Out of the four considered combinations, they determined the best one on the basis of overall performance in scouring, deposition, channel alignment and dredging volume. In a more recent study, Koutrouveli *et al.* (2018) tried to determine the optimal spacing of a series of groynes for maximizing bed shear stress along the main channel and minimizing sidewall shear stress in the groyne field. From their numerical study, they concluded that the spacing between the first four groynes should be small and larger spacing should be used subsequently.

All of the studies referred to above use the trial and error approach for determining the best combination of groynes. In this approach at first a few combinations are chosen and all of them are simulated separately either numerically or experimentally. Finally, their performances are compared in regards to the specified objective/objectives and the best one is then found from the considered scenarios. This technique therefore does not guarantee the best optimal solution as the best one obtained is one of the predefined combinations considered by the modeller. Moreover, getting the best solution mostly depends upon the modeller's experience. The modeller should have adequate experience for choosing the initial probable combinations as well as proper reasoning capability for comparing the performances of them. To avoid such biases, an optimization model is required which can automatically evaluate the optimal combination of groynes for achieving control over a river reach at minimum cost. In this regard, Kalita *et al.* (2014) made an initial effort to determine the optimal combination of groynes by using optimization technique. For this purpose, they formulated a linked simulation–optimization model. They developed the hydrodynamic flow simulation model by solving the two-dimensional (2D) shallow water equations using a finite difference technique. In their optimization model, they minimized the total construction cost of the whole project. They used GA for solving the linked

simulation–optimization model. This model can automatically determine the cost-effective combination of groynes in terms of their number, position and length to have the desired training within a river reach. However, their model has a few shortcomings. First, as their hydrodynamic flow simulation model solves the governing equations in Cartesian coordinate system, the developed model is difficult to use in channel bends. Second, the optimization model developed can place groynes only on one bank of the river. This is not always appropriate, as bank erosion may occur on both the banks for consecutive river bends.

This paper presents a new linked simulation–optimization model, which can automatically determine the cost-effective combination of groynes to prevent bank erosion on any location within a river flow. The flow simulation model is developed by solving the boundary fitted 2D shallow water equations using total variation diminishing (TVD) predictor corrector scheme. The optimization model is formulated in such a way that it can automatically determine the optimal number, lengths and positions of groynes on both the banks of a river. While determining the cost-effective combination, it keeps near bank flow speed to a very low value. In order to solve the linked model, GA, one of the robust optimization techniques is considered in this study.

HYDRODYNAMIC FLOW SIMULATION MODEL

Governing equations

The 2D shallow water equations can be obtained by vertically integrating the Navier–Stokes equations over the depth (Chaudhry 2008). Considering uniform velocity distribution over depth, assuming hydrostatic pressure distribution, neglecting wind shear, ignoring Coriolis acceleration and for small bottom slope, these equations can be written as (Alauddin & Tsujimoto 2012):

$$\frac{\partial S}{\partial t}+\frac{\partial}{\partial x}(hu)+\frac{\partial}{\partial y}(hv)=0 \tag{1}$$

$$\frac{\partial}{\partial t}(hu)+\frac{\partial}{\partial x}(hu^2)+\frac{\partial}{\partial y}(huv)=-gh\frac{\partial S}{\partial x}-\frac{gn^2u\sqrt{(u^2+v^2)}}{h^{\frac{1}{3}}}+\frac{\partial}{\partial x}\left\{v_t\frac{\partial}{\partial x}(hu)\right\}+\frac{\partial}{\partial y}\left\{v_t\frac{\partial}{\partial y}(hu)\right\} \tag{2}$$

$$\frac{\partial}{\partial t}(hv)+\frac{\partial}{\partial x}(huv)+\frac{\partial}{\partial y}(hv^2)=-gh\frac{\partial S}{\partial y}-\frac{gn^2v\sqrt{(u^2+v^2)}}{h^{\frac{1}{3}}}+\frac{\partial}{\partial x}\left\{v_t\frac{\partial}{\partial x}(hv)\right\}+\frac{\partial}{\partial y}\left\{v_t\frac{\partial}{\partial y}(hv)\right\} \tag{3}$$

where S is water stage, h is depth of flow, u, v are depth-averaged velocity components in x and y directions, respectively, g is gravitational aceleration and n is Manning's roughness value. In Equations (2) and (3), v_t is the eddy viscocity due to turbulence and can be found by several empirical equations (Wu *et al.* 2004), such as depth-averaged parabolic eddy viscosity model, modified mixing length model, standard k-ε turbulence model, etc. In this work, v_t is calculated by the simplest but efficient enough depth-averaged parabolic eddy viscosity model (Wu 2007) given by:

$$v_t=\alpha_t h\sqrt{\frac{gn^2}{h^{\frac{1}{3}}}(u^2+v^2)} \tag{4}$$

where α_t is an empirical coefficient between 0.3 and 1.0 (Elder 1959). A constant value of 0.67 is considered for this coefficient throughout the study.

The governing equations presented above are converted to a boundary fitted coordinate system (ξ, η) to make the present model convenient for application in meandering channels and are given as (Anderson *et al.* 1984):

$$\frac{\partial}{\partial t}(JS)+\frac{\partial}{\partial \xi}(huy_\eta-hv.x_\eta)+\frac{\partial}{\partial \eta}(hvx_\xi-huy_\xi)=0 \tag{5}$$

$$\begin{aligned}&\frac{\partial}{\partial t}(Jhu)+\frac{\partial}{\partial \xi}(hu^2y_\eta-huvx_\eta)+\frac{\partial}{\partial \eta}(huvx_\xi-hu^2y_\xi)\\&=-ghy_\eta\frac{\partial S}{\partial \xi}+ghy_\xi\frac{\partial S}{\partial \eta}-J\frac{gn^2u\sqrt{(u^2+v^2)}}{h^{\frac{1}{3}}}\\&+v_t\left\{\begin{array}{l}\frac{1}{J}y_\eta^2\frac{\partial^2}{\partial \xi^2}(hu)-\frac{1}{J}y_\eta y_\xi\frac{\partial^2}{\partial \xi\partial \eta}(hu)\\-\frac{1}{J}y_\xi y_\eta\frac{\partial^2}{\partial \eta\partial \xi}(hu)+\frac{1}{J}y_\xi^2\frac{\partial^2}{\partial \eta^2}(hu)\end{array}\right\}\\&+v_t\left\{\begin{array}{l}\frac{1}{J}x_\eta^2\frac{\partial^2}{\partial \xi^2}(hu)-\frac{1}{J}x_\eta x_\xi\frac{\partial^2}{\partial \xi\partial \eta}(hu)\\-\frac{1}{J}x_\xi x_\eta\frac{\partial^2}{\partial \eta\partial \xi}(hu)+\frac{1}{J}x_\xi^2\frac{\partial^2}{\partial \eta^2}(hu)\end{array}\right\}\end{aligned} \tag{6}$$

$$\frac{\partial}{\partial t}(Jhv)+\frac{\partial}{\partial \xi}(huvy_\eta-hv^2x_\eta)+\frac{\partial}{\partial \eta}(hv^2x_\xi-huvy_\xi)$$
$$=+\mathrm{g}hx_\eta\frac{\partial S}{\partial \xi}-\mathrm{g}hx_\xi\frac{\partial S}{\partial \eta}-J\frac{\mathrm{g}n^2v\sqrt{(u^2+v^2)}}{h^{\frac{1}{3}}}$$
$$+\nu_t\left\{\begin{array}{l}\frac{1}{J}y_\eta^2\frac{\partial^2}{\partial \xi^2}(hv)-\frac{1}{J}y_\eta y_\xi\frac{\partial^2}{\partial \xi\partial \eta}(hv)\\-\frac{1}{J}y_\xi y_\eta\frac{\partial^2}{\partial \eta\partial \xi}(hv)+\frac{1}{J}y_\xi^2\frac{\partial^2}{\partial \eta^2}(hv)\end{array}\right\}$$
$$+\nu_t\left\{\begin{array}{l}\frac{1}{J}x_\eta^2\frac{\partial^2}{\partial \xi^2}(hv)-\frac{1}{J}x_\eta x_\xi\frac{\partial^2}{\partial \xi\partial \eta}(hv)\\-\frac{1}{J}x_\xi x_\eta\frac{\partial^2}{\partial \eta\partial \xi}(hv)+\frac{1}{J}x_\xi^2\frac{\partial^2}{\partial \eta^2}(hv)\end{array}\right\} \quad (7)$$

In Equations (5)–(7), x_ξ, y_ξ, x_η and y_η are the grid transformation coefficients and are determined using central finite difference approximations. J is the Jacobian determinant of grid transformation and given as:

$$J=x_\xi.y_\eta-x_\eta.y_\xi \quad (8)$$

Equations (5)–(7) can be written in matrix form as:

$$\frac{\partial L}{\partial t}+\frac{\partial M}{\partial \xi}+\frac{\partial N}{\partial \eta}=R \quad (9)$$

where

$$L=\left\{\begin{array}{l}JS\\Jhu\\Jhv\end{array}\right\},M=\left\{\begin{array}{l}huy_\eta-hvx_\eta\\hu^2y_\eta-huvx_\eta\\huvy_\eta-hv^2x_\eta\end{array}\right\},N=\left\{\begin{array}{l}hvx_\xi-huy_\xi\\huvx_\xi-hu^2y_\xi\\hv^2x_\xi-huvy_\xi\end{array}\right\},$$

$$R=\left\{\begin{array}{l}0\\-\mathrm{g}hy_\eta\frac{\partial S}{\partial \xi}+\mathrm{g}hy_\xi\frac{\partial S}{\partial \eta}-J\frac{\mathrm{g}n^2u\sqrt{(u^2+v^2)}}{h^{\frac{1}{3}}}+A\\+\mathrm{g}hx_\eta\frac{\partial S}{\partial \xi}-\mathrm{g}hx_\xi\frac{\partial S}{\partial \eta}-J\frac{\mathrm{g}n^2v\sqrt{(u^2+v^2)}}{h^{\frac{1}{3}}}+B\end{array}\right\} \quad (10)$$

where

$$A=\nu_t\left\{\begin{array}{l}\frac{1}{J}y_\eta^2\frac{\partial^2}{\partial \xi^2}(hu)-\frac{1}{J}y_\eta y_\xi\frac{\partial^2}{\partial \xi\partial \eta}(hu)\\-\frac{1}{J}y_\xi y_\eta\frac{\partial^2}{\partial \eta\partial \xi}(hu)+\frac{1}{J}y_\xi^2\frac{\partial^2}{\partial \eta^2}(hu)\end{array}\right\}$$
$$+\nu_t\left\{\begin{array}{l}\frac{1}{J}x_\eta^2\frac{\partial^2}{\partial \xi^2}(hu)-\frac{1}{J}x_\eta x_\xi\frac{\partial^2}{\partial \xi\partial \eta}(hu)\\-\frac{1}{J}x_\xi x_\eta\frac{\partial^2}{\partial \eta\partial \xi}(hu)+\frac{1}{J}x_\xi^2\frac{\partial^2}{\partial \eta^2}(hu)\end{array}\right\} \quad (11)$$

$$B=\nu_t\left\{\begin{array}{l}\frac{1}{J}y_\eta^2\frac{\partial^2}{\partial \xi^2}(hv)-\frac{1}{J}y_\eta y_\xi\frac{\partial^2}{\partial \xi\partial \eta}(hv)\\-\frac{1}{J}y_\xi y_\eta\frac{\partial^2}{\partial \eta\partial \xi}(hv)+\frac{1}{J}y_\xi^2\frac{\partial^2}{\partial \eta^2}(hv)\end{array}\right\}$$
$$+\nu_t\left\{\begin{array}{l}\frac{1}{J}x_\eta^2\frac{\partial^2}{\partial \xi^2}(hv)-\frac{1}{J}x_\eta x_\xi\frac{\partial^2}{\partial \xi\partial \eta}(hv)\\-\frac{1}{J}x_\xi x_\eta\frac{\partial^2}{\partial \eta\partial \xi}(hv)+\frac{1}{J}x_\xi^2\frac{\partial^2}{\partial \eta^2}(hv)\end{array}\right\} \quad (12)$$

TVD MacCormack scheme

The governing equations presented by Equation (9), represented by the vectors in Equations (10)–(12) are a set of mixed hyperbolic partial differential equations. Since this set of equations does not have any closed form analytical solution, it is mostly solved using numerical techniques. Out of the various methods, MacCormack predictor corrector (MacCormack 1969) scheme is one of the excellent and widely used methods for this type of equation. This finite difference-based explicit scheme is second order accurate and also has the capacity to capture the shock front. In this method the solution advances in two steps, namely, predictor and corrector steps. Many researchers (Fennema & Chaudhry 1990; Liang *et al.* 2006; Bellos & Tsakiris 2016; Kalita 2016) solved the above governing equations in Cartesian coordinate system using MacCormack scheme for simulation of unsteady open channel flow. Similarly, some investigators (Bellos *et al.* 1991; Bhallamudi & Chaudhry 1992; Liang *et al.* 2007) also attempted these equations in a boundary fitted coordinate system using the same numerical technique. However, turbulence closure terms are ignored in all of these models. In the present work, effort is given to solve these governing shallow water equations along with the turbulence terms, in a boundary fitted coordinate system. Even though the MacCormack scheme is very simple and easy to understand, it faces the dispersion error problem (Anderson *et al.* 1984) near steep gradients. In order to remove this error one excellent process is TVD method. In TVD technique one extra term is added after the traditional corrector step of the standard MacCormack scheme. In the present work, the TVD method proposed by Davis (1984) is used in conjunction with the standard MacCormack scheme. The main advantage of this TVD version is that it does not require any characteristic transformation (Liang *et al.* 2007).

In the present work, the 2D problem is first split (Strang 1968) into a sequence of two one-dimensional (1D) problems. These 1D problems are then solved using the standard predictor corrector steps sequentially for four times and at each time the TVD step is added. Using the operator splitting technique, Equation (9) is rearranged into:

$$\frac{\partial L}{\partial t}+\frac{\partial M}{\partial \xi}=P \tag{13}$$

and

$$\frac{\partial L}{\partial t}+\frac{\partial N}{\partial \eta}=Q \tag{14}$$

where

$$P=\begin{Bmatrix} 0 \\ -ghy_\eta\dfrac{\partial S}{\partial \xi}-J\dfrac{gn^2u\sqrt{(u^2+v^2)}}{h^{\frac{1}{3}}}+C1 \\ ghx_\eta\dfrac{\partial S}{\partial \xi}+D1 \end{Bmatrix},$$

$$Q=\begin{Bmatrix} 0 \\ ghy_\xi\dfrac{\partial S}{\partial \eta}+E1 \\ -ghx_\xi\dfrac{\partial S}{\partial \eta}-J\dfrac{gn^2v\sqrt{(u^2+v^2)}}{h^{\frac{1}{3}}}+F1 \end{Bmatrix} \tag{15}$$

where

$$C1=\nu_t\left\{\frac{1}{J}y_\eta^2\frac{\partial^2}{\partial\xi^2}(hu)-\frac{1}{J}y_\eta y_\xi\frac{\partial^2}{\partial\xi\partial\eta}(hu)\right\}+\nu_t\left\{\frac{1}{J}x_\eta^2\frac{\partial^2}{\partial\xi^2}(hu)-\frac{1}{J}x_\eta x_\xi\frac{\partial^2}{\partial\xi\partial\eta}(hu)\right\} \tag{16}$$

$$D1=\nu_t\left\{\frac{1}{J}y_\eta^2\frac{\partial^2}{\partial\xi^2}(hv)-\frac{1}{J}y_\eta y_\xi\frac{\partial^2}{\partial\xi\partial\eta}(hv)\right\}+\nu_t\left\{\frac{1}{J}x_\eta^2\frac{\partial^2}{\partial\xi^2}(hv)-\frac{1}{J}x_\eta x_\xi\frac{\partial^2}{\partial\xi\partial\eta}(hv)\right\} \tag{17}$$

$$E1=\nu_t\left\{-\frac{1}{J}y_\xi y_\eta\frac{\partial^2}{\partial\eta\partial\xi}(hu)+\frac{1}{J}y_\xi^2\frac{\partial^2}{\partial\eta^2}(hu)\right\}+\nu_t\left\{-\frac{1}{J}x_\xi x_\eta\frac{\partial^2}{\partial\eta\partial\xi}(hu)+\frac{1}{J}x_\xi^2\frac{\partial^2}{\partial\eta^2}(hu)\right\} \tag{18}$$

$$F1=\nu_t\left\{-\frac{1}{J}y_\xi y_\eta\frac{\partial^2}{\partial\eta\partial\xi}(hv)+\frac{1}{J}y_\xi^2\frac{\partial^2}{\partial\eta^2}(hv)\right\}+\nu_t\left\{-\frac{1}{J}x_\xi x_\eta\frac{\partial^2}{\partial\eta\partial\xi}(hv)+\frac{1}{J}x_\xi^2\frac{\partial^2}{\partial\eta^2}(hv)\right\} \tag{19}$$

The finite difference sequence followed for the 1D problems (Equations (13) and (14)) are given as:

$$L_{i,j}^{k+1}=l_\xi l_\eta l_\eta l_\xi L_{i,j}^k \tag{20}$$

where l_ξ and l_η are the 1D finite difference operators along ξ and η directions, respectively. The subscript and superscript of L represent the spatial grid levels and temporal grid levels, respectively. At first, Equation (13) is solved in ξ direction and the values of the primitive flow variables are found. Using these values, Equation (14) is solved in η direction. After that, the solution is carried out in η direction, followed by the solution in ξ direction. The finite difference discretization along with the TVD step for the first sweep for Equation (13) is given by:

$$L_i^p=L_i^k-\frac{\Delta t}{\Delta\xi}(M_i^k-M_{i-1}^k)+\Delta tP_i^k \tag{21}$$

$$L_i^c=L_i^k-\frac{\Delta t}{\Delta\xi}(M_{i+1}^p-M_i^p)+\Delta tP_i^p \tag{22}$$

$$L_i^{k+1}=\frac{1}{2}(L_i^p+L_i^c)L_i^k+\{G(r_i^+)+G(r_{i+1}^-)\}\Delta L_{i+\frac{1}{2}}^k-\{G(r_{i-1}^+)+G(r_i^-)\}\Delta L_{i-\frac{1}{2}}^k \tag{23}$$

where $\Delta\xi$ is the spatial grid spacing in ξ direction designated by the subscript i, Δt is the time step designated by the superscript k, superscripts p and c stands for predicted and corrected values, respectively.

In Equation (23):

$$\Delta L_{i+\frac{1}{2}}^k=L_{i+1}^k-L_i^k,\ \ \Delta L_{i-\frac{1}{2}}^k=L_i^k-L_{i-1}^k \tag{24}$$

$$r_i^+=\frac{\Delta S_{i-\frac{1}{2}}^k.\Delta S_{i+\frac{1}{2}}^k+\Delta(hu)_{i-\frac{1}{2}}^k.\Delta(hu)_{i+\frac{1}{2}}^k+\Delta(hv)_{i-\frac{1}{2}}^k.\Delta(hv)_{i+\frac{1}{2}}^k}{\Delta S_{i+\frac{1}{2}}^k.\Delta S_{i+\frac{1}{2}}^k+\Delta(hu)_{i+\frac{1}{2}}^k.\Delta(hu)_{i+\frac{1}{2}}^k+\Delta(hv)_{i+\frac{1}{2}}^k.\Delta(hv)_{i+\frac{1}{2}}^k} \tag{25}$$

$$r_i^+=\frac{\Delta S_{i-\frac{1}{2}}^k.\Delta S_{i+\frac{1}{2}}^k+\Delta(hu)_{i-\frac{1}{2}}^k.\Delta(hu)_{i+\frac{1}{2}}^k+\Delta(hv)_{i-\frac{1}{2}}^k.\Delta(hv)_{i+\frac{1}{2}}^k}{\Delta S_{i-\frac{1}{2}}^k.\Delta S_{i-\frac{1}{2}}^k+\Delta(hu)_{i-\frac{1}{2}}^k.\Delta(hu)_{i-\frac{1}{2}}^k+\Delta(hv)_{i-\frac{1}{2}}^k.\Delta(hv)_{i-\frac{1}{2}}^k} \tag{26}$$

The expression for G () in Equation (23) is considered as:

$$G(f)=0.5\times c\times\{1-\varnothing(f)\} \tag{27}$$

where the flux limiter function $\varnothing(f)$ is given by:

$$\varnothing(f) = \max\{0, \min(2f, 1)\} \tag{28}$$

and the value of variable c is:

$$c = Cr \times (1 - Cr) \text{if } Cr \leq 0.5$$
$$= 0.25 \text{ if } Cr > 0.5 \tag{29}$$

with Cr being the local Courant number given by:

$$Cr = \frac{\left(|u| + \sqrt{gh}\right)\Delta t}{\Delta x} \tag{30}$$

In Equation (28), several flux limiter functions such as minmod limiter, monotonic limiter, superbee limiter, MUSCL limiter, etc. may be used. Wang *et al.* (2000) did a comparative analysis for all these limiters and observed that minmod limiter could provide very good results and therefore the present study also considers the same.

Initial and boundary conditions

In order to solve the above finite difference approximated equations, the initial condition is required from where the simulation starts. Similarly, proper boundary conditions are also required at each computational boundary. In the present model, all the analyses are carried out considering constant discharge in the river. By considering uniform flow condition in the river, the initial values of all the three primitive flow variables are calculated from the considered constant discharge. These values constitute the initial condition for the hydrodynamic model. In regards to boundary condition, the same constant discharge is applied at the upstream boundary and the corresponding uniform flow depth is used at the downstream boundary. The solid boundaries (i.e., river bank and the groyne wall) are simulated as free slip boundary (Anderson *et al.* 1984).

Stability of the model

The numerical model developed here is based on explicit approach and therefore the value of Δt should be chosen such that the Courant–Friedrichs–Lewy (CFL) criterion is satisfied. According to this criterion, the value of Δt should be chosen such that the value of Cr given in Equation (30) is less than unity for numerical stability.

Validation of the model

The present numerical model is validated with the experimental data of Rajaratnam & Nwachukwu (1983) for their test run A1. They conducted this experiment in a straight rectangular flume of length 37 m and width 0.914 m. They used an aluminium plate of thickness of 0.003 m and of length 0.15 m, as groyne structure. In the present work, an area extending from 1.8 m upstream to 3.6 m downstream of the groyne is considered for simulation (Yazdi *et al.* 2010). The whole flow domain is discretized into finite difference grids of size 92 × 43. The grids are packed near the vicinity of the groyne to capture the high gradient of flow parameters. The lowest and the highest grid spacing in x direction is 0.0015 m and 0.2 m, respectively. Similarly in y direction, these values are 0.01 m and 0.05 m, respectively. Manning's roughness is considered as 0.01 $m^{-1/3}s$ for the smooth channel. A flow discharge of 0.045 m^3/s and a water depth of 0.189 m are specified as upstream and downstream boundaries, respectively. The same discharge value is also used as initial condition in the numerical model. The time step is specified as 0.0006 second leading to Courant number of 0.72.

Starting from a uniform flow state for the given discharge, the numerical model is run up to steady state by considering the time step as iteration number. Figure 1 represents the steady-state solution in terms of the velocity vector. The velocity vectors clearly show the recirculation zone developed downstream of the groyne, originated due to the pressure difference. The same figure also shows that the recirculation zone is finishing at a distance of 3.6 m from the upstream, which is exactly the same as that of the experimental case. Apart from the recirculation zone extent comparison, non-dimensional resultant flow velocities are also compared with the experimental results. For this purpose, the resultant flow velocity (W) is non-dimensionalized with respect to free upstream flow velocity (u_0) of 0.253 m/s. Figure 2 shows the comparison of numerical and experimental non-dimensional flow velocities on four longitudinal sections at distances of 0.15 m, 0.225 m, 0.4 m and 0.6 m from the right bank. These comparisons also show the good matching of both

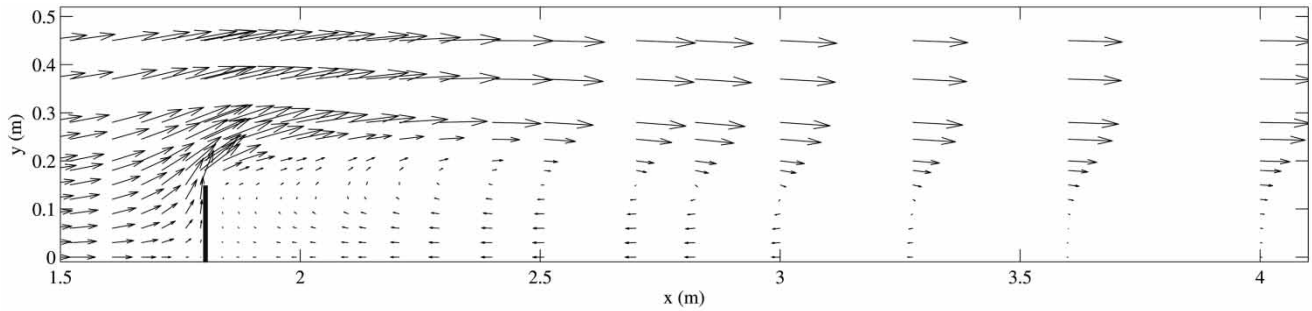

Figure 1 | Velocity vector plot for the steady-state solution.

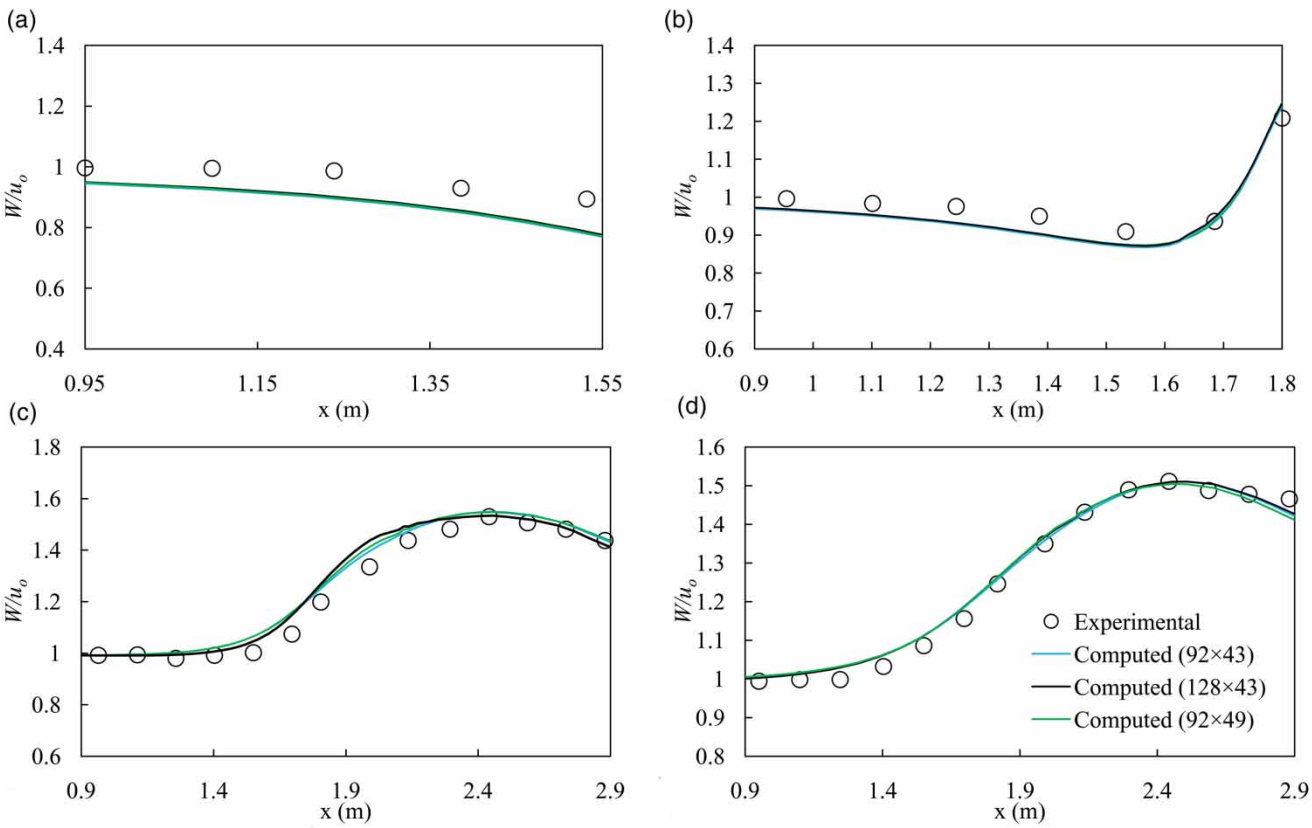

Figure 2 | Comparison of computed and experimental flow velocities at: (a) 0.15 m; (b) 0.225 m; (c) 0.4 m; (d) 0.6 m.

the results. In order to study the mesh effect on the result, two more meshes are created by changing the grid spacings in both x and y directions. These meshes are 128×43 and 92×49. Comparison of experimental and numerical non-dimensional velocities for these meshes is also shown in Figure 2. It may be observed that results for all the three meshes are exactly the same and establish the independency of the result on mesh size. From all of these comparisons it can be concluded that the present numerical model behaves excellently for flow simulation around groynes.

OPTIMIZATION MODEL FORMULATION

Whenever a series of groynes is constructed on a river bank, a low flow zone is developed within the groyne

field (Alauddin & Tsujimoto 2012). Consequently, the shear stress developed at the soil boundary is reduced and the bank erosion is mitigated (Hanson & Cook 1997; Koutrouveli *et al.* 2018). Therefore, the groyne system should be designed in such a way that can lead to desired low speed on the groyne field at least possible cost. The present optimization model is formulated using these concepts of low speed of water and least cost of the project. The proposed optimization model minimizes the total construction cost of the whole groyne system, at the same time achieving the desired low speed on any location within a river flow. Three different formulations are proposed to tackle different types of field problems and are as follows.

Formulation I

In this formulation, it is assumed that the fund available is unlimited and any number of groynes can be constructed to save a vulnerable river bank. The optimization model here determines the optimal number, length and position of the groynes, to achieve a desired target speed on a predefined near bank area. By keeping the target speed value on the near bank area to a lower limit, it is assumed that the bank can be saved on that area. The optimization formulation can be written as:

$$\text{Min } C = \sum_{GN=1}^{N} (GLL + GLR) \times \text{p} \tag{31}$$

Subject to,

$$U \leq \theta \tag{32}$$

$$GLL_{min} \leq GLL \leq GLL_{max}, GLR_{min} \leq GLR \leq GLR_{max} \tag{33}$$

$$GPL_{min} \leq GPL \leq GPL_{max}, \ GPR_{min} \leq GPR \leq GPR_{max} \tag{34}$$

where C is the total construction cost of the groyne system, GN is the required number of groynes to be constructed, GLL and GLR are the groyne lengths on the left and the right bank, respectively, p is the construction cost per metre length of groyne, GPL and GPR are the groyne positions on the left and the right bank, respectively. It may be mentioned here that the value of p is strictly dependent upon the site condition and the respective value should be chosen accordingly. Equations (33) and (34) represent the upper and lower limits of groyne length and positions, respectively, U is maximum flow speed of water on the predefined near bank area (obtained from the numerical model) and θ is the predefined target speed value. From the above formulation it may be observed that the groyne position does not have any direct effect on the project cost. However, the optimal position of groynes can help in fulfilling the constraint of target speed (Equation (32)). Regarding the determination of optimal number of groynes, the model is initially given a high number of possible groynes. The model is formulated in such a way that it can automatically determine the number of groynes actually required by allocating zero length to the rest of the groynes.

Formulation II

In practice, sometimes construction of a groyne is not possible on each point throughout the bank line due to the existence of some unstable bank portion. In order to handle this specific case, formulation II is proposed in this work. In this formulation, position of the groynes are already fixed on both the banks. The optimization model finds the length of the groynes required on these positions to achieve the desired target speed on the predefined near bank area. In this case, also the required number of groynes is the number of groynes having non-zero length. The optimization problem formulation can be written as:

$$\text{Min } C = \sum_{GN=1}^{N} (GLL + GLR) \times \text{p} \tag{35}$$

Subject to,

$$U \leq \theta \tag{36}$$

$$GLL_{min} \leq GLL \leq GLL_{max}, GLR_{min} \leq GLR \leq GLR_{max} \tag{37}$$

where the variables C, GN, GLL, GLR, p, U and θ represent the same as that of formulation I.

Formulation III

This formulation incorporates the issue of fund shortage for the project. It is assumed that the fund available for the project is limited and therefore the number and the length of the groynes are already finalized with the available fund. Since the number and length of the groynes are already fixed, the cost of the project cannot be minimized further. Rather, the optimization function minimizes the speed of water on the predefined area, by finding their optimal locations. The optimization formulation can be written as:

$$\text{Min } U \tag{38}$$

Subject to,

$$GPL_{min} \leq GPL \leq GPL_{max},\ GPR_{min} \leq GPR \leq GPR_{max} \tag{39}$$

where the variables U, GPL and GPR represent the same as that of formulation I.

GENETIC ALGORITHM FOR THE LINKED SIMULATION-OPTIMIZATION MODEL

Once the optimization problems have been formulated, they need to be linked with the hydrodynamic flow simulation model. This is because the value of U can be obtained only after running the simulation model with the groynes generated by the optimization model. In order to link these two separate models, one promising method is linked simulation–optimization technique. The linked simulation–optimization is a very popular technique and is used by several researchers in various hydrological problems such as sustainable ground water management (Boddula & Eldho 2018), groundwater contamination source determination (Ayvaz 2016), optimal groyne combination determination (Kalita *et al.* 2014), etc. Due to this robustness, the present work also uses the linked simulation–optimization approach.

In order to solve the stated linked simulation–optimization model, several optimization techniques are available in the literature. However, for this type of nonlinear and non-convex problem, it is very difficult to obtain the global optimal solution using the traditional optimization methods (Kalita *et al.* 2014). GA is one of the excellent evolutionary techniques in this regard. GA is a nonlinear search and optimization technique based on the natural evolution process and inspired by survival of fittest principle (Holland 1975). GA does not rely on mathematical properties of the objective function such as differentiability and continuity and this makes it more robust and applicable (Goldberg 1989). GA starts with a randomly generated set of initial populations (chromosomes), with each population assigned with some fitness value. The populations may be represented by either using binary number (binary string) or using real number. However, using binary strings with accuracy 1, GA can easily be used for integer variable problems (Kalita *et al.* 2014). Iterations (generations) are then carried out to refine the populations to increase their fitness values. These iterations are carried out until some convergence is achieved. Three main operators, such as selection, crossover and mutations are carried out within each generation of GA to modify the populations to have maximized fitness. Readers are directed to studies (Davis 1991; Michalewicz 1992; Deb 1999) for better understanding of the whole GA process. Jung & Karney (2006) reported that GA can even sometimes solve problems where traditional methods fail. Some noticeable achievements using GA in diverse hydrological problems are rainfall–runoff modelling (Chlumecky *et al.* 2017), multi-use reservoir operation (Chang *et al.* 2010), parameter estimation in flood routing model (Zhang *et al.* 2017), etc. Due to the various advantages associated with GA, the present work also uses GA for solving the developed optimization formulations.

Figure 3 is a flow chart illustrating the proposed linked simulation–optimization model. The model starts by randomly generating a set of initial populations within the bounds. The initial populations here are the lengths and positions of the initially considered large number of groynes. The objective function (cost of the project) is then determined with the considered set of groynes. After that, the simulation model is run with a modified bathymetry of the river incorporating the groynes, up to steady state. The maximum speed on the proposed area (U) is then found and used in the optimization model to check the constraint. The initial set of populations is then taken through the genetic operators, i.e., selection, crossover and mutation. This

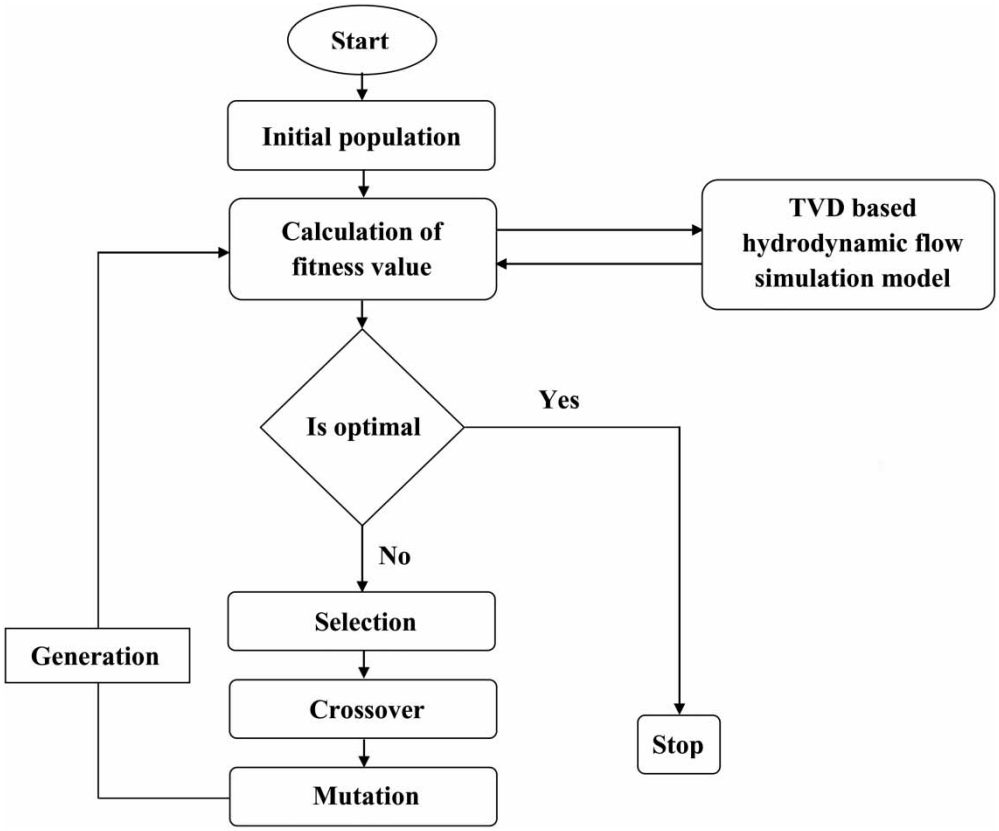

Figure 3 | Schematic flow chart of the proposed linked simulation–optimization model.

whole process is then repeated for the given number of generations. Finally, the model yields a result vector, of which the first half elements represent the optimal lengths of the required groynes and the second half represents their corresponding optimal positions. As stated earlier, the required number of groynes at this step are the groynes having non-zero length. The steps given in the preceding section are for formulation I. In formulation II, initial population means the randomly generated lengths of the groynes at the fixed locations. Initial population in formulation III is positions of the already specified groynes of known lengths.

In the present model, the decision variables are number, length and position of groyne. The number of groyne is always an integer numeral. The length and position of groyne generated by the optimization model are numerical numbers and, accordingly, the river bed is elevated on these grid numbers in the simulation model. The hydrodynamic simulation model is developed in such a way that it automatically considers these elevated grids as groynes and subsequently uses the boundary conditions. Therefore, these numbers will also have to be integer in nature. Eventually it can be observed that all the decision variables are integer in nature and that is why binary strings with accuracy of 1 are used to represent the variables. Tournament selection method is used for the selection operator (Nield *et al.* 2005). The crossover and the mutation probabilities are considered as 0.8 and 0.005, respectively (Goldberg 1989; Srinivas & Patnaik 1994). All the optimization problems are run for 100 generations.

APPLICATION OF THE PROPOSED MODEL

The proposed model is applied in two different test cases to test its applicability. In the first case, it is used to determine the optimal combination of groynes required on one of the banks of a hypothetical straight channel. In the second case, a hypothetical meandering channel is chosen and the

proposed model is used to determine the optimal combination of groynes required on both the banks.

Hypothetical straight channel

The considered channel is 800 m long and 200 m wide with Manning's n value of 0.035 $m^{-1/3}s$. The bottom slope of the channel is considered as 1:2,000. A flow discharge of 1,000 m^3/s is applied at the upstream boundary and the corresponding uniform flow depth of 3.49 is applied at the downstream boundary. The flow domain is discretized into 81×21 grids, leading to a uniform grid spacing of 10 m in both directions. The time step is chosen such that the value of Cr is 0.7. An area extending from nodes 1 to 3 in transverse direction and 31 to 51 in longitudinal direction is considered as the low speed zone. The flow channel along with the proposed low speed zone near the right bank is shown in Figure 4(a). The low speed zone is chosen merely just to check the applicability of the proposed model, even though it may be anywhere within the flow domain. The developed linked simulation–optimization model is used to determine the cost-effective combination of groynes (in terms of GN, GLR and GPR) to achieve low target speed value on this area.

The length of groyne is generally kept within 20% of the channel width (Seed 1997). In the present case, the width of the channel is 200 m and, consequently, the maximum length of the groyne is fixed as 40 m. This 40 m long groyne can be represented by five nodes in the transverse direction of flow as each grid has a grid spacing of 10 m. Therefore the values of GLR_{min} and GLR_{max} are specified as 0 and 5, respectively. The variable GLR is thus encoded with a string length of 3 to have the results in terms of integer numeral. Regarding the position of the groyne, it is assumed that groynes may be placed on upstream, downstream and also within the low speed zone. Therefore, GPR_{min} and GPR_{max} are specified as nodes 21 and 61, respectively, in the longitudinal direction of flow. As this difference of position limits is 40, the variable GPR is encoded with a binary string of length 6.

Hypothetical bend channel

The applicability of the present model in problems requiring groynes on both the river banks is tested by considering a hypothetical channel bend. Figure 4(b) shows the flow channel composed of two 90° bends and three straight tangents. The inner radius of the bends is 350 m. The lengths of the approach, middle and exit channels are 295.2 m, 147.6 m and 295.2 m, respectively. The width and bed slope of the channel are considered as 240 m and 1:2,000, respectively. The upstream flow discharge is 1,200 m^3/s, while the downstream flow depth is 3.48 m. The grid selected is 121×21 and the Cr value is set as 0.7. Manning's roughness is considered as 0.035 $m^{-1/3}s$ for the hypothetical channel. As this case contains both concave

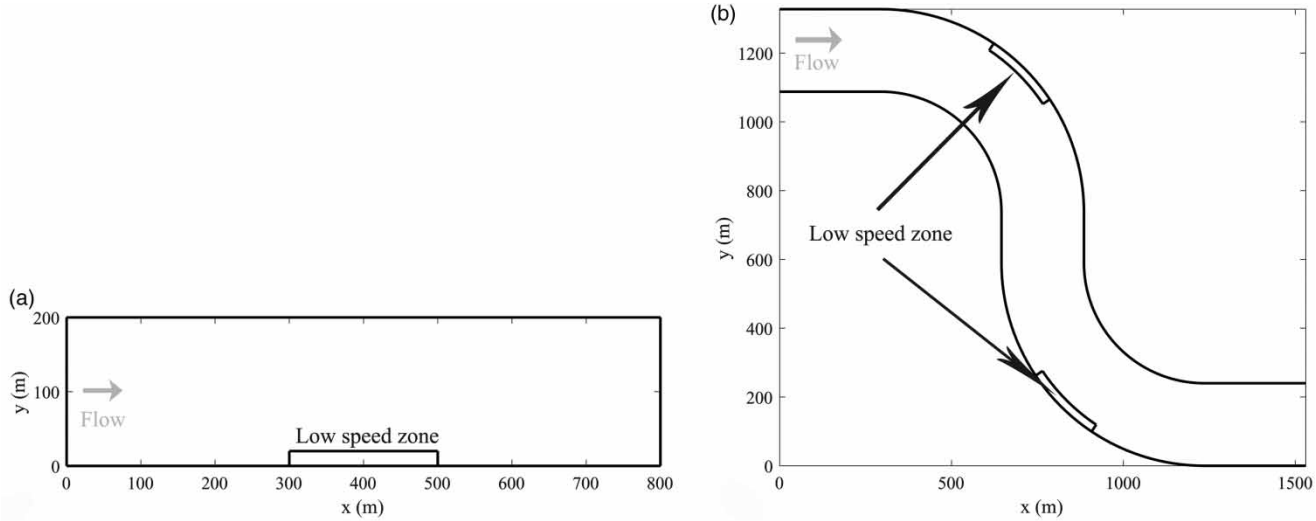

Figure 4 | Study areas with proposed low speed zones: (a) hypothetical straight channel; (b) hypothetical channel bend.

and convex curves, it can be easily understood that the left bank is more vulnerable to erosion in the first curve and similarly the right bank in the second curve. As such, two low speed zones are considered for this flow channel and are shown in Figure 4(b). Extent of the first zone is from nodes 1 to 3 in the transverse direction and 32 to 42 in the flow direction. Similarly, for the second low speed zone, these extensions are from nodes 19 to 21 and 80 to 90, in transverse and flow directions, respectively. The proposed linked simulation–optimization model finds the cost-effective combination of groynes (in terms of *GN*, *GLR*, *GPR*, *GLL* and *GPL*) to achieve low target speed on these areas.

The lower and upper limits of *GLL* and *GLR* are fixed as 0 and 5, respectively. GPL_{min}, GPL_{max}, GPR_{min} and GPR_{max} are set as nodes 17, 57, 65 and 105, respectively. With a view to get these variables in integer format, *GPL* and *GPR* are encoded with a binary string of length 6, while *GLL* and *GLR* are with a binary string of length 3.

RESULTS AND DISCUSSION

The proposed GA-based linked simulation–optimization model is applied for both the channels, with all three formulations and the results obtained are presented in the subsequent sections.

Straight channel

Formulation I minimizes the total construction cost of the groyne project to attain a target speed value of 0.2 m/s on the predefined low speed zone. In order to initiate the computation, five probable groynes are considered within the position limits. For these groynes, the associated variables are their positions and lengths. Therefore, the total number of variables is ten. An initial population of size 100, ten times the variable size is considered. The optimization model results in two numbers of groynes (*GN*) to achieve the stated target speed value. The optimal lengths (*GLR*) of these two groynes are 3 and 4. These two integer numbers actually represent the number of grids occupied by the groynes in the hydrodynamic flow domain. As the transverse grid spacing considered in this case is 10 m, these two numerical values, in fact, represent groynes of length 30 and 40 m, respectively. The corresponding optimal positions (*GPR*) for these two groynes are found to be nodes 31 and 44, respectively, from the upstream boundary. These two nodes represent two chainage values from the upstream boundary, i.e., 300 and 430 m, respectively. Figure 5(a) shows the

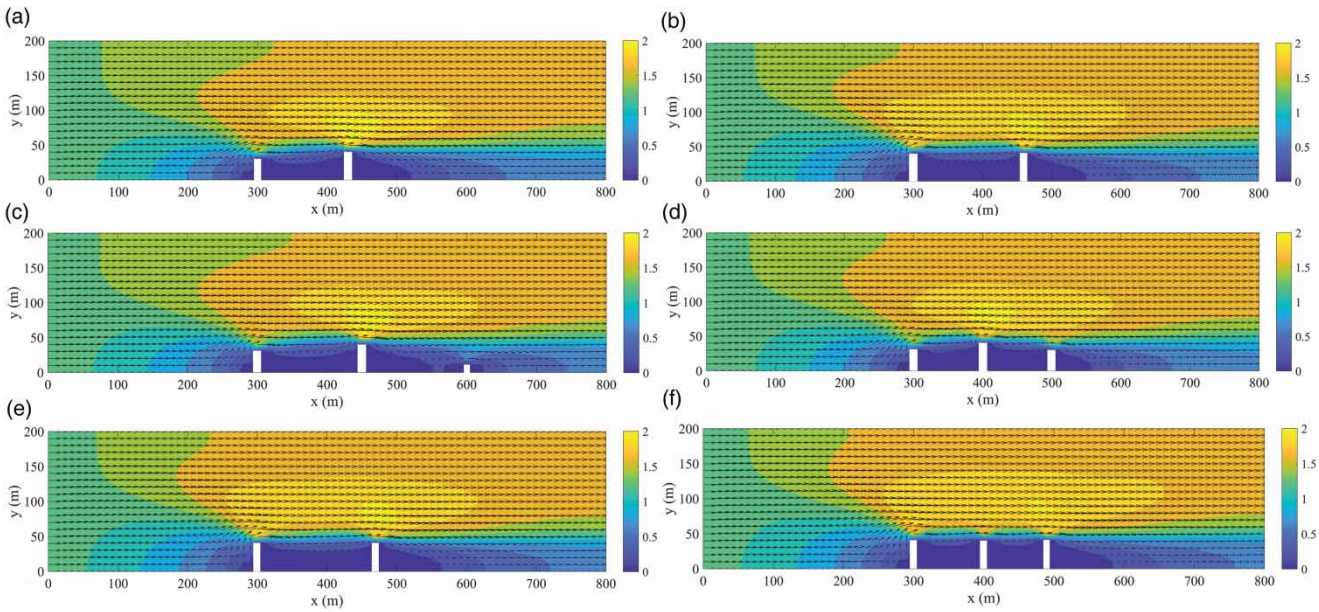

Figure 5 | Hydrodynamic solution in terms of velocity vector and speed contour map (m/s) with optimal combination of groynes for the straight channel: (a) formulation I with $\theta = 0.2$ m/s; (b) formulation I with $\theta = 0.1$ m/s; (c) formulation II with $\theta = 0.2$ m/s; (d) formulation II with $\theta = 0.1$ m/s; (e) formulation III with two groynes; (f) formulation III with three groynes.

steady-state hydrodynamic solution with the optimal groyne combination. The deflected pattern of the flow due to the groynes is well reproduced by the vector plot. The length of the velocity vectors are found to be less within the groyne field showing low speed there. Speed contour map also reveals low speed on the predefined area near the southern bank. With these groynes the cost of the whole project is found to be 70p. The values of *GLR* and *GPR* for this case are provided in Table 1. The developed model is then used for another target speed of 0.1 m/s. In this case also the model results in requirements of two groynes, but both of them now become 40 m long. Table 1 may be further referred to for the details of the optimal combinations for this case. Figure 5(b) shows the velocity vector plot along with the speed contour map for this groyne combination. The project cost in this case increases to 80p due to increase in the groyne length.

In formulation II, the positions of groynes are fixed on the bank. These positions may be anywhere on the bank. However, for simplicity, they are considered uniformly distributed within the position limits. Initially fixed positions are chainages 200, 250, 300, 350, 400, 450, 500, 550 and 600 m. For these positions the corresponding variable is their lengths and therefore the total number of variables is 9. An initial population of 90 is considered. In order to have a comparison with formulation I, formulation II is run with same target speed values considered in formulation I. The proposed model shows that out of these nine positions, groynes need to be constructed on three positions to achieve these target speeds. The optimal lengths and positions of these groynes for both the target speeds are listed in Table 1. The corresponding project costs are also included in the same table. Figure 5(c) and 5(d) show the corresponding hydrodynamic solutions.

Two trials are done in formulation III by changing the groyne numbers. The first trial assumes two groynes and the second trial assumes three groynes. In both the trials the lengths of the groynes are fixed as 40 m. The optimal positions provided by the model for these groynes are given in Table 1. With two groynes the speed can lower to 0.109 m/s on the predefined zone and with three groynes this value is found to be 0.022 m/s. The respective hydrodynamic solutions are shown in Figure 5(e) and 5(f).

A few interesting points are observed from the preceding results. In formulations I and II, as the target speed reduces, the lengths of the required groynes increases. This eventually increases the hypothetical project cost considered in this work. This is also as intuitively expected. Comparison of results for the same target speeds between formulations I and II reveals that formulation I can provide better results compared to formulation II. In formulation I, the proposed

Table 1 | Optimal groyne combination for the test channels

Channel type	Formulation	Target speed (θ) (m/s)	Groyne number (*GN*)	Groyne length on left bank in terms of grid occupied (*GLL*)	Groyne length on left bank in terms of metre (*GLL*)	Groyne length on right bank in terms of grid occupied (*GLR*)	Groyne length on right bank in terms of metre (*GLR*)	Groyne position on left bank in terms of node number (*GPL*)	Groyne position on left bank in terms of metre (*GPL*)	Groyne position on right bank in terms of node number (*GPR*)	Groyne position on right bank in terms of metre (*GPR*)	*C*
Straight	I	0.2	2	–	–	3, 4	30, 40	–	–	31, 44	300, 430	70p
		0.1	2	–	–	4, 4	40, 40	–	–	31, 47	300, 460	80p
	II	0.2	3	–	–	3, 4, 1	30, 40, 10	–	–	31, 46, 61	300, 450, 600	80p
		0.1	3	–	–	3, 4, 3	30, 40, 30	–	–	31, 41, 51	300, 400, 500	1,00p
	III	–	2	–	–	4, 4	40, 40	–	–	31, 48	300, 470	80p
		–	3	–	–	4, 4, 4	40, 40, 40	–	–	31, 41, 50	300, 400, 490	1,20p
Bend	I	0.3	5	2, 2, 2	24, 24, 24	3, 2	36, 24	30, 37, 42	–	79, 88	–	132p
		0.2	4	3, 3	36, 36	4, 2	48, 24	32, 40	–	80, 89	–	144p
	II	0.3	6	1, 3, 2	12, 36, 24	1, 3, 2	12, 36, 24	25, 33, 41	–	73, 81, 89	–	144p
		0.2	6	1, 3, 3	12, 36, 36	1, 4, 2	12, 48, 24	25, 33, 41	–	73, 81, 89	–	168p
	III	–	4	4, 4	48, 48	4, 4	48, 48	32, 39	–	80, 88	–	192p
		–	6	4, 4, 4	48, 48, 48	4, 4, 4	48, 48, 48	32, 38, 42	–	80, 85, 90	–	288p

model is free to search the optimal location. However, in formulation II, the locations are prefixed, which may not be the optimal locations. As such, the model is more general in terms of formulation I than formulation II and therefore provides better results with formulation I. In formulation III, increase in groyne number leads to more reduction in flow speed on the predefined zone, as expected. Variables *GLR* and *GPR* are represented both in grid/node numbers as well as metres. It is an easy task here because of uniform grid spacing throughout the computational domain.

Bend channel

Formulation I is used for two target speed values of 0.3 m/s and 0.2 m/s in the bend channel. As this channel contains two vulnerable banks, the proposed model finds the optimal groyne combination on both the banks. The computation starts with five probable groynes on each bank leading to a total of ten groynes. The initial population considered is 200. In order to achieve the target speed of 0.3 m/s, the optimization model results in the requirement of five groynes. Out of these, three groynes of length 24 m each need to be constructed on the left bank at nodes 30, 37 and 42. The remaining two groynes, of length 36 and 24 m, are to be constructed on the right bank at nodes 79 and 88, respectively. The cost of the project with these groynes is found to be 132p. Figure 6(a) shows the hydrodynamic solution in terms of velocity vector and speed contour map. Due to the groynes, the velocity vectors are getting deflected away from the vulnerable bank. Speed contour map reveals low speed on the groyne field. With target speed of 0.2 m/s, the optimization model results in four groynes, with two on each bank. The length required for both the groynes is 36 m on the left bank, with optimal positions of 32 and 40. Similarly, on the right bank, these lengths are found to be 48 and 24 m along with optimal positions of 80 and 89, respectively. Figure 6(b) shows the velocity vector and speed contour map for the steady-state solution. The enhanced project cost is found to be 144p. The optimal groyne arrangements for this formulation are provided in Table 2.

Formulation II also uses the same target speed values, i.e., 0.3 m/s and 0.2 m/s. Initial fixed locations for placing the groynes on the left bank are nodes 17, 25, 33, 41, 49 and 57, along the flow direction. Similarly, on the right bank, these nodes are 65, 73, 81, 89, 97 and 105. An initial population of 120 is considered in this case. The proposed model reveals that groynes are to be constructed at three positions on each bank, for both the target speeds. The optimal lengths and positions for these groynes, along with the corresponding project costs, are given in Table 2. The resultant hydrodynamic solutions with these groynes are depicted in Figure 6(c) and 6(d).

Formulation III is tested for two trials by changing the groyne numbers. The first trial considers two groynes of length 40 m each and the second trial assumes three the same, on each bank. Optimal positions provided by the model for these groynes along with the respective project costs are listed in Table 2. Using four groynes, the flow speed that can be achieved on the predefined zones is 0.096 m/s, and by six groynes this value is found to be 0.017 m/s. The respective hydrodynamic solutions are shown in Figure 6(e) and 6(f).

This test case also reveals similar observations like the earlier one, i.e., formulation I can produces better results in comparison to formulation II, due to robust formulation. The project cost is also found to be increased with decrease in target speed for formulations I and II. Formulation III reveals that with a larger number of groynes less speed can be achieved on the predefined area. Regarding the variables *GLL* and *GLR*, the results are expressed both in terms of grid occupied as well as metre. This is possible because of uniform grid spacing of 12 m in the transverse direction. Variables *GPL* and *GPR* are represented with node numbers only. No chainage values can be used as the channel is curved in nature. One possible solution for this problem can be the use of nondimensional distances from the upstream boundary. However, this is not much discussed here as the authors believe that it is not the general solution for the problem. The plan form of natural rivers rarely follows standard geometric shape and therefore the grid generated will also be non-uniform throughout the domain. Therefore, if the present model is applied in natural rivers, it will be very difficult to convert the resultant groyne length and groyne position into metre unit. In that case, first of all, the resultant hydrodynamic plot may be geo-referenced with the help of some available tools like ArcGIS,

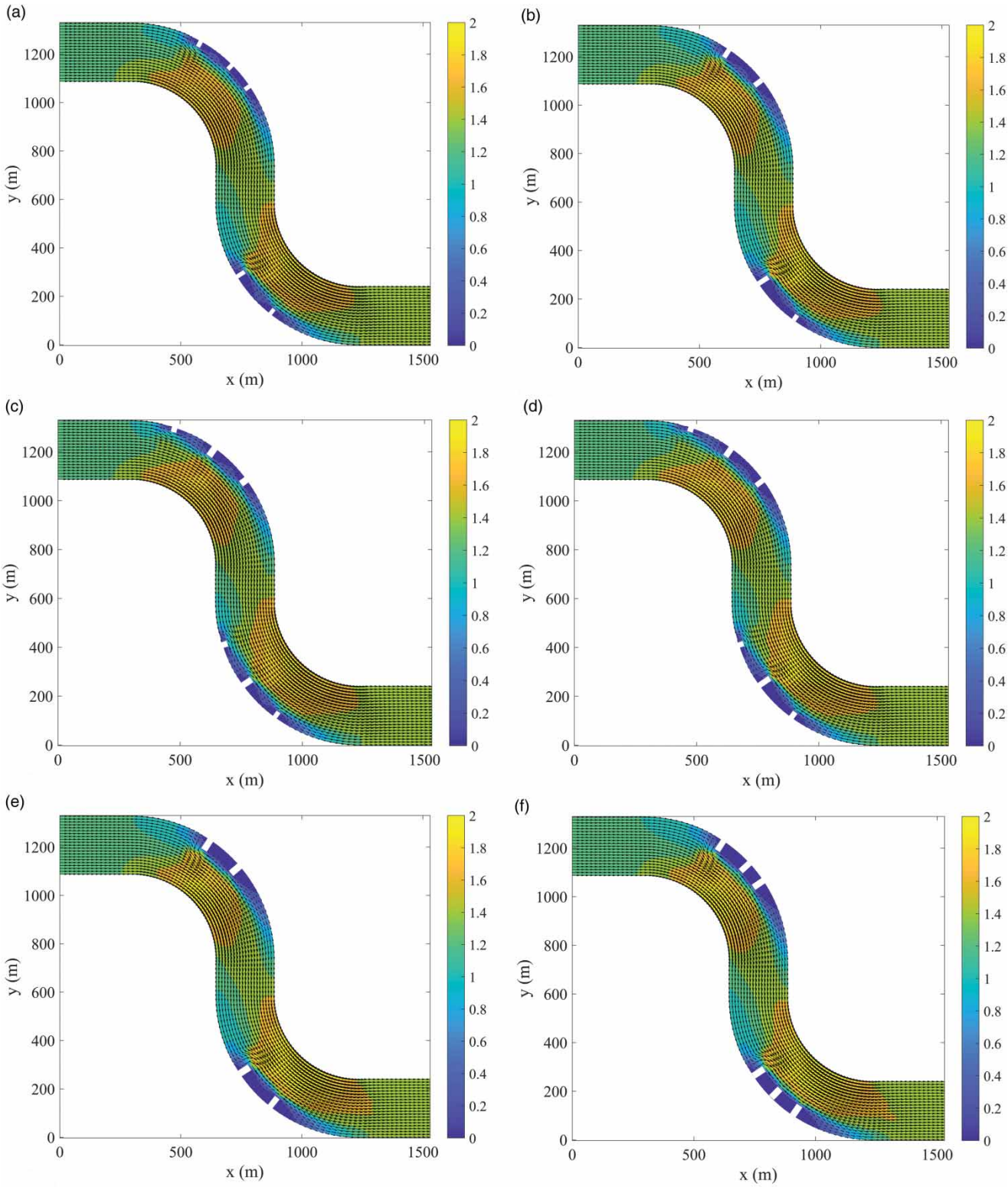

Figure 6 | Hydrodynamic solution in terms of velocity vector and speed contour map (m/s) with optimal combination of groynes for the bend channel: (a) formulation I with $\theta = 0.3$ m/s; (b) formulation I with $\theta = 0.2$ m/s; (c) formulation II with $\theta = 0.3$ m/s; (d) formulation II with $\theta = 0.2$ m/s; (e) formulation III with four groynes; (f) formulation III with six groynes.

Table 2 | Computational time requirements

Channel type	Formulation	Trials	Initial population considered	Computational time required (hr)
Straight	I	1 and 2	100	6.5
	II	1 and 2	90	5.4
	III	1	20	1.5
		2	30	2
Bend	I	1 and 2	200	37
	II	1 and 2	120	19.5
	III	1	40	8.4
		2	60	12.6

ERDAS IMAGINE, etc. After that, the resultant groyne number and positions can easily be obtained in metres from the geo-referenced map.

Computational efficiency

All the test problems presented in the earlier sections are run on a Windows 7 based Intel Core i7 CPU with 3.4 GHz Processor Desktop computer. Matlab is used for programming the same. Computational time required for all the test cases are found out and tabulated in Table 2. This table clearly shows that the present model requires more computational time when the initial population size is large. Apart from the initial population, computational efficiency also depends upon the number of finite difference nodes considered in the hydrodynamic model. The bend channel is discretized into 9,801 nodes in comparison to 1,701 nodes considered for the straight channel. This leads to requirements of more computational time for all the formulations in the bend channel compared to the straight one.

CONCLUSIONS

Groynes are one of the most widely used river training structures for prevention of bank erosion. They are often constructed in series to prevent vulnerable river banks. As they require a huge amount of investment cost, this study deals with determination of a cost-effective combination of groynes to exert control over a river reach. A linked simulation–optimization model is developed in this regard by linking a hydrodynamic simulation model with a GA-based optimization model. The 2D shallow water equations are solved using TVD-based MacCormack predictor corrector scheme. The optimization model is formulated in three different ways (formulations I, II and III) to tackle different types of actual field problems. In order to handle the integer nature of the variables, the proposed linked simulation–optimization model is solved using binary coded GA. The applicability of the proposed model is tested in two different test cases, including a straight channel, as well as a meandering channel. For both the channels, as the target speed reduces, the corresponding project cost increases to achieve the stated target speeds. Formulation I is found to be better compared to formulation II. It is also observed that the proposed model can efficiently find the optimal locations if the groyne number and lengths are known already.

One of the disadvantages of the present model is its computational time requirement. During the reported computational time, the model attempts numerous combinations. Trying all these combinations experimentally or numerically otherwise would have taken much more time. Yet the authors believe that computational time requirement is high, specifically for the bend channel. Another disadvantage of the proposed model is its inability to handle oriented groynes (attracting or deflecting types).

The authors believe that the present work may be extended in many ways. A few future scopes of the work are summarized in the following points:

1. The present model may be applied to some natural river with the availability of flow and bathymetric data.
2. A sediment transport model may be incorporated into the simulation model. In that case, sediment deposition amount can directly be specified as a constraint, rather than setting some low speed value.
3. The orientation of the groyne may also be incorporated as another variable in the optimization problem. The effect of orientation can then be studied.
4. Although the GA parameters are chosen here based on the criteria available from the standard literature, a sensitivity analysis for them may also be carried out to see their effects on the project cost.
5. Some recent and advanced optimization techniques may also be tested to increase the computational efficiency.

ACKNOWLEDGEMENTS

The authors would like to thank Prof. Rajib Kumar Bhattacharjya, Indian Institute of Technology Guwahati, for providing a copy of the Binary Coded Genetic Algorithm (BGA) code and for the permission to use it in the present work.

REFERENCES

Ahmad, M. 1953 Experiments on design and behavior of spur dikes. In: *Proceedings of Conference on International Hydraulic Convention, ASCE*, New York, USA, pp. 145–159.

Alauddin, M. & Tsujimoto, T. 2012 Optimum configuration of groynes for stabilization of alluvial rivers with fine sediments. *Int. J. Sediment Res.* **27** (2), 158–167.

Anderson, D. A., Tannehill, J. D. & Pletcher, R. H. 1984 *Computational Fluid Mechanics and Heat Transfer*. McGraw-Hill, New York, USA.

Ayvaz, M. T. 2016 A hybrid simulation–optimization approach for solving the areal groundwater pollution source identification problems. *J. Hydrol.* **538**, 161–176.

Bellos, C. V. & Tsakiris, G. 2016 A hybrid method for flood simulation in small catchments combining hydrodynamic and hydrological techniques. *J. Hydrol.* **540**, 331–339.

Bellos, C. V., Soulis, J. V. & Sakkas, J. G. 1991 Computation of two-dimensional dam-break induced flows. *Adv. Water Resour.* **14** (1), 31–41.

Bhallamudi, S. M. & Chaudhry, M. H. 1992 Computation of flows in open-channel transitions. *J. Hydraul. Res.* **30** (1), 77–93.

Boddula, S. & Eldho, T. I. 2018 Groundwater management using a new coupled model of meshless local Petrov-Galerkin method and modified artificial bee colony algorithm. *Computat. Geosci.* **22** (3), 657–675.

Chang, L. C., Chang, F. J., Wang, K. W. & Dai, S. Y. 2010 Constrained genetic algorithms for optimizing multi-use reservoir operation. *J. Hydrol.* **390**, 66–74.

Chaudhry, M. H. 2008 *Open Channel Flow*, 2nd edn. Prentice-Hall, Englewood Cliffs, NJ, USA.

Chlumecky, M., Buchtele, J. & Richta, K. 2017 Application of random number generators in genetic algorithms to improve rainfall-runoff modelling. *J. Hydrol.* **553**, 350–355.

Davis, S. F. 1984 *TVD Finite Difference Schemes and Artificial Viscosity*. ICASE Report No. 84-20.

Davis, L. 1991 *Handbook of Genetic Algorithms*. Van Nostrand Reinhold, New York, USA.

Deb, K. 1999 An introduction to genetic algorithms. *Sadhana* **24**, 293–315.

Duan, J. G. & Nanda, S. K. 2006 Two-dimensional depth-averaged model simulation of suspended sediment concentration distribution in a groyne field. *J. Hydrol.* **327**, 426–437.

Elder, J. W. 1959 The dispersion of marked fluid in turbulent shear flow. *J. Fluid Mech.* **5** (4), 544–560.

Fennema, R. J. & Chaudhry, M. H. 1990 Explicit methods for 2-D transient free-surface flows. *J. Hydraul. Eng.* **116** (8), 1013–1034.

Garde, R. J., Subramanya, K. & Nambudripad, K. D. 1961 Study of scour around spur-dikes. *J. Hydraul. Eng.* **87** (HY6), 23–37.

Glas, M., Glock, K., Tritthart, M., Liedermann, M. & Habersack, H. 2018 Hydrodynamic and morphodynamic sensitivity of a river's main channel to groyne geometry. *J. Hydraul. Res.* **56**, 714–726. doi:10.1080/00221686.2017.1405369.

Goldberg, D. E. 1989 *Genetic Algorithms in Search, Optimization, and Machine Learning*. Addison-Wesley, Boston, MA, USA.

Hakimzadeh, H., Azari, N. & Mehrzad, R. 2012 Experimental study of lateral structural slopes of groynes on scour reduction. In: *Proceedings of Sixth International Conference on Scour and Erosion*, Paris, France, pp. 1035–1040.

Hanson, G. J. & Cook, K. R. 1997 *Development of Excess Shear Stress Parameters for Circular jet Testing*. ASAE, Paper No. 972227, ASAE, St. Joseph, MI, USA. doi:10.1002/esp.1657.

Holland, J. H. 1975 *Adaptation in Natural and Artificial Systems*. University of Michigan Press, Ann Arbor, MI, USA.

Jeon, J., Lee, J. Y. & Kang, S. 2018 Experimental investigation of three-dimensional flow structure and turbulent flow mechanisms around a nonsubmerged spur dike with a low length-to-depth ratio. *Water Resour. Res.* **54** (5), 3530–3566. doi:10.1029/2017WR021582.

Juez, J. C., Buehlmann, I., Maechler, G., Schleiss, A. & Franca, M. J. 2018a Transport of suspended sediments under the influence of bank macro-roughness. *Earth Surf. Process. Landf.* **43** (1), 271–284.

Juez, C., Thalmann, M., Schleiss, A. J. & Franca, M. J. 2018b Morphological resilience to flow fluctuations of fine sediment deposits in bank lateral cavities. *Adv. Water Resour.* **115**, 44–59.

Jung, B. S. & Karney, B. W. 2006 Hydraulic optimization of transient protection devices using GA and PSO approaches. *J. Water Resour. Plan. Manage.* **132** (1), 44–52.

Kalita, H. M. 2016 A new total variation diminishing predictor corrector approach for two-dimensional shallow water flow. *Water Resour. Manage.* **30** (4), 1481–1497.

Kalita, H. M., Sarma, A. K. & Bhattacharjya, R. K. 2014 Evaluation of optimal river training work using GA based linked simulation-optimization approach. *Water Resour. Manage.* **28** (8), 2077–2092.

Karmaker, T. & Dutta, S. 2016 Prediction of short-term morphological change in large braided river using 2D numerical model. *J. Hydraul. Eng.* **142** (10), 1–13.

Koutrouveli, T. I., Dimas, A. A., Fourniotis, N. T. & Demetracopoulos, A. C. 2018 Groyne spacing role on the effective control of wall shear stress in open-channel flow. *J. Hydraul. Res.* **57** (2), 167–182. doi:10.1080/00221686.2018.1478895.

Kuhnle, R. A., Alonso, C. V. & Shields, F. D. 2002 Local scour associated with angled spur groynes. *J. Hydraul. Eng.* **128** (12), 1087–1093.

Liang, D., Falconer, R. A. & Lin, B. 2006 Comparison between TVD-MacCormack and ADI-type solvers of the shallow water equations. *Adv. Water Resour.* **29** (12), 1833–1845.

Liang, D., Lin, B. & Falconer, R. A. 2007 A boundary-fitted numerical model for flood routing with shock-capturing capability. *J. Hydrol.* **332**, 477–486.

MacCormack, R. W. 1969 The effect of viscosity in hypervelocity impact cratering. In: *Proceedings of AIAA Hypervelocity Impact Conference*, Cincinnati, OH, USA, pp. 69–354.

McCoy, A., Constantinescu, G. & Weber, L. J. 2008 Numerical investigation of flow hydrodynamics in a channel with a series of groynes. *J. Hydraul. Eng.* **134** (2), 157–172.

Michalewicz, Z. 1992 *Genetic Algorithms + Data Structures = Evolution Programs*. Springer-Verlag, Berlin, Germany.

Mukherjee, A. & Sarma, A. K. 2010 *2D Flow Simulation in Alluvial River Using MIKE Software: A Modeling Approach*. Lambert Academic Publishing, Saarbrucken, Germany.

Nield, J., Walker, D. & Lambert, M. 2005 Two-dimensional equilibrium morphological modelling of a tidal inlet: an entropy based approach. *Ocean Dynam.* **55** (5–6), 549–558.

Ouillon, S. & Dartus, D. 1997 Three-dimensional computation of flow around groyne. *J. Hydraul. Eng.* **123** (11), 962–970.

Ouro, P., Cea, L., Ramirez, L. & Nogueira, X. 2016 An immersed boundary method for unstructured meshes in depth averaged shallow water models. *Int. J. Numer. Meth. Fluids* **81** (11), 672–688.

Qin, J., Zhong, D., Wua, T. & Wua, L. 2017 Sediment exchange between groin fields and main-stream. *Adv. Water Resour.* **108**, 44–54.

Rajaratnam, N. & Nwachukwu, A. 1983 Flow near groin-like structures. *J. Hydraul. Eng.* **109** (3), 463–480.

Seed, D. J. 1997 *Guidelines on the Geometry of Groynes for River Training*. Report SR 493, HR Wallingford, Wallingford, UK.

Srinivas, M. & Patnaik, L. M. 1994 Adaptive probabilities of crossover and mutation in genetic algorithms. *IEEE T. Syst. Man Cy.* **24** (4), 656–667.

Strang, G. 1968 On the construction and comparison of difference scheme. *SIAM J. Numer. Anal.* **5**, 506–517.

Sukhodolov, A. N. 2014 Hydrodynamics of groyne fields in a straight river reach: insight from field experiments. *J. Hydraul. Res.* **52** (1), 105–120.

Sukhodolov, A., Engelhardt, C., Kruger, A. & Bungartz, H. 2004 Case study: turbulent flow and sediment distributions in a groyne field. *J. Hydraul. Eng.* **130** (1), 1–9.

Tingsanchali, T. & Maheswaran, S. 1990 2D depth-averaged flow computation near groyne. *J. Hydraul. Eng.* **116** (1), 71–85.

Tritthart, M., Glas, M., Liedermann, M. & Habersack, H. 2014 Numerical study of morphodynamics and ecological parameters following alternative groyne layouts at the Danube River. In: *Proceedings of 11th International Conference on Hydroscience and Engineering*, Hamburg, Germany, pp. 684–692.

Uijttewaal, W. S. 2005 Effects of groyne layout on the flow in groyne fields: laboratory experiments. *J. Hydraul. Eng.* **131** (9), 782–791.

Wang, J. S., Ni, H. G. & He, Y. S. 2000 Finite-difference TVD scheme for computation of dam-break problems. *J. Hydraul. Eng.* **126** (4), 253–262.

Wu, W. 2007 *Computational River Dynamics*. Taylor and Francis, London, UK.

Wu, W. M., Wang, P. & Chiba, N. 2004 Comparison of 5 depth average 2D turbulence models for river flows. *Arch. Hydro. Eng. Environ. Mech.* **51** (2), 183–200.

Yazdi, J., Sarkardeh, H., Azamathulla, H. M. & Ghani, A. A. 2010 3D simulation of flow around a single spur dike with free surface flow. *Int. J. River Basin Manage.* **8** (1), 55–62.

Yossef, M. F. M. & de Vriend, H. 2010 Sediment exchange between a river and its groyne fields: mobile-bed experiment. *J. Hydraul. Eng.* **136** (9), 610–625.

Zhang, S., Kang, L., Zhou, L. & Guo, X. 2017 A new modified nonlinear Muskingum model and its parameter estimation using the adaptive genetic algorithm. *Hydrol. Res.* **48** (1), 17–27.

First received 6 March 2019; accepted in revised form 3 June 2019. Available online 15 July 2019